Chapter 6

COUPLING LIQUID CRYSTAL ORIENTATION TO AN ASSOCIATING POLYMER NETWORK: MULTIPLE RELAXATION PROCESSES IN LIQUID CRYSTALLINE PHYSICAL GELS

The work presented in this chapter was done jointly with Rafael Verduzco and in collaboration with Sam Sprunt (Dept. of Physics, Kent State University) and Peter Palffy-Muhoray (Liquid Crystal Institute, Kent State University). Rafael Verduzco synthesized the side-on polymers (names ending with “BB”) and we collected the light scattering data together in Sam Sprunt’s lab. Sam Sprunt and Peter Palffy-Muhoray contributed to the experimental design and interpretation of the results. We thank Prof. Sprunt’s students, Sunil Sharma and Krishna Neupane, for their help with light scattering experiments.

6.1 Introduction

Dispersing a physically crosslinked network of associating polymer in a small-molecule nematic liquid crystal (LC) solvent couples the network's elasticity with the LC's orientational order, giving rise to electro-optic and mechano-optic properties not present in either material alone. For example, the gel can be aligned into a uniform monodomain simply by applying mechanical shear, and the gel's optical response is fast enough to track a 1 kHz alternating electric field.[1] This coupling between the polymer network and the LC solvent also gives rise to rich dynamic processes in LC physical gels. The physically associated network is capable of dynamic restructuring: on short time scales the network is unchanging, as though it were chemically crosslinked, but the slow process of breaking and reforming crosslinks allows the network to rearrange on long time scales. The orientation of the LC solvent fluctuates with thermal energy and these fluctuations are translated to the network via liquid crystalline side-groups covalently attached to the polymer chains.

The dynamics of LC orientation fluctuations has been extensively studied using dynamic light scattering.[2] When the LC orientation, described by the nematic director, ***n***, fluctuates away from its equilibrium orientation, $\boldsymbol{n_0}$, the resulting distortion can be expressed as the sum of a splay, twist, and bend distortion (Figure 6.1) and the elastic penalty is expressed by the Frank elastic free energy per unit volume, F_V:

$$F_V = \tfrac{1}{2}\left[K_1(\nabla\cdot\mathbf{n})^2 + K_2(\mathbf{n}\cdot(\nabla\times\mathbf{n}))^2 + K_3\left|\mathbf{n}\times(\nabla\times\mathbf{n})\right|^2\right] \tag{6.1}$$

where K_1, K_2, and K_3 are the splay, twist, and bend elastic constants, respectively.[3] Frank elasticity drives the director to return to $\boldsymbol{n_0}$ at a rate, τ_ν^{-1}, determined by the ratio of K_ν to the LC's corresponding anisotropic viscosity η_{splay}, η_{twist}, and η_{bend}:

$$\tau_\nu^{-1} = \frac{K_\nu}{\eta_\nu}q^2, \quad \nu = \text{splay, twist, or bend,}^{[2,4]} \tag{6.2}$$

where q is the magnitude of the scattering vector. Choosing the correct geometry can isolate light scattering from fluctuations of splay, twist, and bend distortions in a nematic LC[2] (Figure 6.2) and the time correlation of the scattered light reveals the dynamics of the distortion's relaxation.

Coupling of LC order to a polymer network has previously been accomplished by chemically crosslinking polymers bearing covalently attached liquid crystalline side groups to create a solvent-free LC elastomer, as reviewed by Warner and Terentjev.[5] The theory of nematic LC elastomers[5-9] predicts the network to provide a restoring torque to director fluctuations, in addition to Frank elasticity, which is a function of the anisotropy of the network's polymer chains. Despite the existence of extensive theory, there exists only one experimental investigation of director dynamics in an LC elastomer.[10] This is due, in part, to the difficulty in preparing uniformly aligned monodomain elastomers that are suitable for dynamic light scattering experiments.

LC physical gels are ideal candidates for dynamic light scattering experiments because they are relatively easy to align. A triblock copolymer having random-coil polymer endblocks (polystyrene, PS) and a side-group liquid crystal polymer (SGLCP) midblock self-assembles in nematic LC solvent to create a physical gel.[1, 11] When the solvent is heated to the isotropic phase, the endblocks become soluble and the network dissolves. Cooling a PS-SGLCP-PS triblock copolymer solution from the isotropic to the nematic phase in the presence of a biasing electromagnetic field causes the gel to form in an aligned solvent and provides an optically uniform monodomain. These gels are similar to nematic elastomers in that mechanical strain is coupled to LC order,[12] but they are orders of magnitude softer by virtue of their solvent content: the modulus of an LC physical gel is approximately 10^2 Pa[11] while the modulus of an LC elastomer is typically greater than 10^5 Pa.[10] The network elasticity in an LC gel is, therefore, comparable to the Frank elasticity of a nematic LC ($\sim 10^2 - 10^3$ Pa on ~1 μm length scales),[3] in contrast to LC elastomers where Frank elasticity is orders of magnitude less than network elasticity.

The dynamics of director fluctuations in LC gels and, for the purposes of comparison, analogous side-group liquid crystal polymer (SGLCP) solutions are explored here using dynamic light scattering from uniform monodomains. Both network elasticity and Frank elasticity contribute to relaxation dynamics, and the network's ability to rearrange with time contributes an additional process for director relaxation. In qualitative agreement with the theory of nematic elastomers, gel relaxation dynamics are found to be dependent on the anisotropy of the network chains.

6.2 Experimental

6.2.1 Materials

Two different triblock copolymers having random coil endblocks and a side-group liquid crystal polymer (SGLCP) midblock were synthesized (Figure 6.3) along with two analogous SGLCP homopolymers (Figure 6.4). An anionically polymerized poly[styrene-b-(1,2-butadiene)- b-styrene] (57 kg/mol PS, 146 kg/mol PB, 67 kg/mol PS) triblock copolymer was purchased from Polymer Source (Montreal, Quebec) and functionalized with end-on (SiCB4) mesogens according to the methods described in Appendix A. Side-on (SiBB) mesogens were attached to the same prepolymer by Rafael Verduzco.[13] An anionically polymerized, 63 kg/mol 1,2-polybutadiene prepolymer provided by Steve Smith of Proctor and Gamble, Inc. was used to make the homopolymers. The characteristics of these four polymers are summarized in Table 6.1 and the details of characterization of end-on polymers are given in Appendix A.

Solutions of polymers in the nematic LC 4-pentyl-4′-cyanobiphenyl (5CB, purchased and used as received from TCI America) were prepared by dissolving the polymer and 5CB together in dichloromethane (DCM), then evaporating the DCM under a stream of air followed by drying in vacuum overnight.

6.2.2 Methods

Solutions of polymer in 5CB were loaded into cells consisting of glass plates separated by 4, 9, or 25 μm spacers. Cells having 4 or 9 μm gaps were purchased from LC Vision (Boulder, CO) and have SiO_2 alignment layers for homogeneous (planar) alignment. Cells having a 25 μm gap were purchased from EHC (Japan) and have rubbed polyimide alignment layers for homogeneous alignment. All three cell types have 5 mm x 5 mm transparent indium-tin oxide (ITO) electrodes in their centers. Cells were filled with polymer / LC solutions by capillary action; homopolymer solutions readily flowed in at room temperature and triblock gels flowed readily when heated above the gel point (35 °C for 5 wt % 1100ABASiCB4 and 33 °C for 5 wt % 1400ABASiBB). Homopolymer solutions spontaneously aligned into a monodomain under the influence of the alignment layers. Gels were aligned into a homogeneous monodomain (LC director parallel to the cell surface) by heating them above the gel point then slowly cooling them inside the bore of an 8 T NMR magnet. Alternatively, gels were aligned into homeotropic monodomains (LC director perpendicular to the cell surface) by heating them above the gel point then cooling while applying a 15 V_{rms} potential difference to the ITO electrodes.

Aligned samples were mounted in a temperature controlled oven with optical access that was stabilized to better than ± 0.01 °C and illuminated with a focused, polarized 20 mW HeNe laser (wavelength λ = 633 nm) incident perpendicular to the cell surface. The incident polarization was vertical, orthogonal to the horizontal scattering plane. Monodomain LC samples were placed in the beam oriented so their director was either parallel to the incident polarization (vertical, V), perpendicular to both the incident polarization and the incident beam (horizontal, H), or parallel to the incident beam (parallel, P) (Figure 6.2). Depolarized light scattering was collected at various scattering angles, θ_s, with the optical scattering vector $\boldsymbol{q}$ ($|\boldsymbol{q}| = q = 4\pi n/\lambda \sin(\theta_s/2)$, where $n \approx 1.55$ is the sample's refractive index) lying in the horizontal plane. The time correlation of the scattered intensity ($g_2(t) = \langle I(q,0)I(q,t)\rangle$) was recorded in the homodyne regime. The resulting intensity autocorrelation functions were normalized by their maximum value, typically 1.95.

Prior to initiating a time correlation experiment, the sample position was adjusted to find a well-aligned region of the sample that minimized the static intensity of the scattered light. Monodomains of homopolymer solutions were highly uniform and required little adjustment. On the other hand, it was more difficult to achieve high-quality monodomains with gels, and more sample adjustment was required prior to each experiment.

On small (< 100 nm) length scales, the gels have a heterogeneous structure that consists of a LC midblock dissolved in LC and phase-separated endblocks swollen with LC.

Significantly, the length scales probed by the experiment are large enough that the system can be considered homogeneous. The light scattering experiments probe length scales ranging between 350 nm (q = 0.018 nm^{-1}) and 2.9 μm (q = 0.002 nm^{-1}). The data may be interpreted on the basis of a uniform material because the length scale of the spatial fluctuations that scatter light are much greater than the length scale of a single micelle.

In some samples, the intensity autocorrelation function did not decay completely even after several hours. Due to the large number of experiments, all samples could not be independently verified for ergodicity. However, selected samples that were chosen to verify ergodicity did manifest a complete decay of the intensity autocorrelation function after a sufficiently long time, up to several weeks.

6.3 Results

6.3.1 Comparison of Gels to Homopolymer Solutions

The relaxation dynamics of liquid crystalline gels are qualitatively different from those of homopolymer solutions or 5CB alone. Pure 5CB exhibits a single, exponential relaxation that fully decays on time scales on the order of 10^{-3} s. Homopolymer solutions behave the same way but the relaxation is shifted towards longer times (10^{-2} - 10^{-1} s). In contrast to both of these, correlations in gels decay non-exponentially and often relax over much longer time scales (> 1 s) (Figure 6.5). In some cases there are two distinct relaxation processes observed; the correlation function nearly overlaps that of the homopolymer solution at short times, but decays slowly at long times (Figure 6.5a).

The degree to which relaxation is slowed in homopolymer solutions relative to pure 5CB depends on the scattering geometry. End-on homopolymer (5 wt % 490HSiCB4) slows relaxation more in the H geometry than in V (Figure 6.5a and b). Side-on homopolymer (5 wt % HiBB) has the opposite effect, slowing relaxation more strongly in the V geometry (Figure 6.5c and d). Anisotropy of the relaxation dynamics is also observed in gels; end-on gels (5 wt % 1100ABASiCB4) have longer-lived correlations in the H geometry and side-on gels in the V geometry (5% 1400ABASiBB) (Figure 6.6). The correlation functions of end-on gels overlap those of end-on homopolymers at short times (Figure 6.5a and b). In the case of side-on gels, the short time relaxation is slower than the homopolymer in the H geometry (Figure 6.5c) and faster in the V geometry (Figure 6.5d).

6.3.2 Comparison of End-On and Side-On Gels

Examining the correlation functions of gels at a variety of scattering angles further demonstrates anisotropy in their relaxation dynamics: both the qualitative shape of the correlation functions and the time scales for relaxation are dependent on the scattering geometry (H or V). The time correlation functions from the end-on gel strongly deviate from single exponential decay at all scattering angles in the H geometry with crossover from fast relaxation to slow relaxation occurring between ~10^{-3} and 10^{-2} s (Figure 6.6a). In the V geometry relaxation closely resembles a single exponential, albeit a stretched exponential, for $\theta_s \geq 30°$ and transitions to relaxation by two processes for $\theta_s < 30°$ (Figure 6.6b). Correlations in the end-on gel are significantly longer-lived in the H geometry than in the V; over the dynamic range studied here, correlation functions in the H geometry do not decay to a baseline of $g_2(t) = 1$ when θ_s is less than ~30° but complete decay is observed at all scattering angles in the V geometry. These trends are reversed in the side-on gel where the relaxation is clearly non-exponential for all scattering angles in the V geometry (Figure 6.6d) but closely resembles a stretched exponential for $\theta_s \geq 16°$ in the H geometry (Figure 6.6c). Long-lived correlations are evident in the V geometry, but in the H geometry the correlation functions completely decay to $g_2(t) = 1$, except at $\theta_s = 8°$. Unlike the end-on gel there is no clear inflection point signaling a crossover from a fast relaxation process to a slow relaxation process in the side-on gel. Instead, the correlation functions in the V geometry are highly stretched to long times.

The sense of the dynamical anisotropy in the gels is identical to that of the homopolymer solutions: the end-on gel has slower dynamics in the bend (H) geometry and the side-on gel has slower dynamics in the splay (V) geometry. The relative contribution of the fast and slow processes is also dependent on the scattering geometry with the slow process playing a more prominent role in the geometry where dynamics are slowest. The relative contribution of the processes is independent of the scattering angle in side-on gels, but in end-on gels the slow process becomes more prominent at smaller angles.

6.3.3 *q*-Dependence of the Relaxation Dynamics

The scaling of relaxation rate with q is revealed by plotting a series of correlation functions at different scattering angles versus rescaled delay time, $t^R = t\,(\sin(\theta_s)/\sin(\theta_{s,0}))^2$, where $\theta_{s,0}$ is a reference angle of $\theta_s = 8°$, thus collapsing them onto a single curve when the relaxation rate depends on q^2. Correlation functions from end-on (Figure 6.7a and b) and side-on on (Figure 6.8a and b) homopolymer solutions superimpose well with this rescaling, but such is not always the case with gels. Correlation functions from end-on gels in the V geometry superimpose well when $\theta_s \geq 30°$. At smaller scattering angles they superimpose well at short times ($t^R < 10^{-2}$ s) but deviate towards higher values of $g_2(t)$ at longer times (Figure 6.7d). The H geometry is similar; correlation functions superimpose well at large scattering angles, but deviate at smaller θ_s (Figure 6.7c). In side-on gels, the correlation functions are found to superimpose well at all scattering angles in both H and V geometries, the only exception being when $\theta_s = 8°$ in the H geometry (Figure 6.8c and d).

Comparing the time scale for relaxation of the gels to that of the corresponding homopolymer solutions shows that the gel slows relaxation in one scattering geometry more strongly than the other. The time scale for complete loss of correlation ($g_2(t) = 1$) is approximately the same for end-on gel and homopolymer solution at $\theta_s < 22°$ in the V geometry ($t^R \approx 10^{-1}$ s) (Figure 6.7b and d), but the gel has much longer-lived correlations ($t^R \approx 10^3$ s) in the H geometry when compared to the homopolymer solution (Figure 6.7a and c). Opposite to what is observed for end-on polymers, the time scale for complete loss of correlation in side-on gel is approximately equal to that of the side-on homopolymer solution ($t^R \approx 10^{-2} – 10^{-1}$ s) in the H geometry (Figure 6.8a and c), but is shifted to much longer time scales in the V geometry ($t^R \approx 10^3$ s) (Figure 6.8b and d).

6.3.4 Concentration Dependence of the Relaxation Dynamics

The time correlation functions from solutions of end-on triblock copolymers are qualitatively different above and below the gel point (~ 5 wt % polymer) (Figure 6.9). A solution of 1 wt % 1100ABASiCB4 in 5CB has a single, exponential relaxation similar in shape to an end-on homopolymer solution. Above the gel point the shape of the correlation function is relatively insensitive to concentration and the dynamics get slower as concentration is increased; correlations are longer-lived in 15 wt % 1100ABASiCB4 than 5 wt % 1100ABASiCB4.

6.3.5 Temperature Dependence of the Relaxation Dynamics

The dynamics of the end-on homopolymer solution and gel are relatively insensitive to changes in temperature. Time correlation functions are virtually superimposable in the temperature range from 25.0 to 33.5 °C (Figure 6.10). In contrast, director relaxation in side-on polymer solutions gets faster as temperature is increased (Figure 6.11). Most dramatically, the relaxation rate of 5 wt % side-on homopolymer in the V geometry increases by almost two orders of magnitude as temperature is increased from 25.0 to 33.5 °C (Figure 6.11b). In the H geometry, however, there is no observable change in this temperature range (Figure 6.11a). Increasing the temperature of the side-on gel has the strongest effect on long-time relaxation dynamics; correlation functions are shifted toward shorter times at higher temperatures, especially in the H geometry (Figure 6.11c). Examining the entire range of scattering angles makes temperature-induced changes in side-on polymer solutions more evident (Figure 6.12). At the highest temperature studied (33.5 °C), homopolymer correlation functions are shifted towards smaller times in the V geometry, but unchanged in the H geometry (Figure 6.12a and b) relative to the data at 25 °C (Figure 6.8a and b). The correlation functions from side-on gels in the H geometry at 31.5 °C in the H geometry more closely resemble a single exponential decay and are shifted towards shorter times relative to the 25 °C data (Figure 6.12c and Figure 6.8c). In the V geometry there is a similar shift and change in shape for correlation functions at $\theta_s \geq 30°$, but when $\theta_s \leq 22°$, the correlation functions are dramatically different from those at high angle: they do not superimpose with the $(\sin(\theta_s)/\sin(\theta_{s,0}))^2$ rescaling and correlations persist to longer time scales (Figure 6.12d).

6.3.6 Relaxation Dynamics of Gels in the P Geometry

Correlation functions from gels in the P geometry have many of the same characteristics observed in the H and V geometries (Figure 6.13). Both gels' correlation functions decay by a combination of a fast and a slow process, the slow process being most prominent at small scattering angles. Long-lived correlations are observed in the side-on gel when $\theta_s \leq 16°$ but are not observed in the end-on gel. The time scale for complete loss of correlation in the P geometry is similar for both gels ($t^R \sim 10^3$ s); for the end-on gel it is similar to that in the H geometry and for the side-on gel it is similar to that in the V geometry.

6.3.7 Fitting Correlation Functions to Determine Relaxation Rates

Correlation functions from homopolymer solutions were fit to the empirical Williams-Watts function:[14, 15]

$$g_2(t) = 1 + \left[e^{-\left(t/\tau\right)^{\beta}} \right]^2 \tag{6.3}$$

where τ is the relaxation rate and $0 < \beta \leq 1$ is a stretching exponent equal to one for purely exponential relaxation. If $\beta < 1$ is assumed to derive from a spectrum of relaxation times, the average relaxation time $<\tau>$ may be calculated:[16]

$$\langle \tau \rangle = \frac{\tau}{\beta} \Gamma\left(\beta^{-1}\right) \tag{6.4}$$

where Γ denotes the Gamma function. Plotting the inverse of $<\tau>$ versus q^2 gives a straight line for homopolymer solutions (Figure 6.14), further demonstrating the expected scaling between relaxation rate and q (equation 6.2). The anisotropy of the relaxation dynamics is evident in the relaxation rates, as well. Relaxation rates of end-on homopolymer solution are faster in the V geometry (Figure 6.14a), but side-on homopolymer solution relaxes faster in the H geometry (Figure 6.14b). The anisotropy is much greater in side-on homopolymer solution; relaxation in the H geometry is about two orders of magnitude faster than in the V geometry whereas the difference is approximately tenfold for end-on homopolymer. The change in the relaxation rates with temperature is negligible in end-on homopolymer solution (Figure 6.14a), but relaxation dynamics get much faster in side-on solution when temperature is increased to 33.5 °C (Figure 6.14b).

The value of the stretching exponent used to fit correlation functions from homopolymer solutions ranged from 0.8 to 1.0, except when fitting end-on solution in the H geometry; in this case the exponent was as low as 0.6. These exponents correlate with the polymers' polydispersities (Table 6.1) and are consistent with a spectrum of relaxation times that would result from a broad distribution of molecular weight. Attempts to use the Williams-Watts function to fit data from gels resulted in β values as low as 0.3, too low to be accounted for by polydispersity alone. Furthermore, the Williams-Watts function fails to describe the two relaxation processes often observed in gels.

6.4 Discussion

6.4.1 Dynamics of Homopolymer Solutions

Director relaxation in solutions of SGLCP homopolymers is a hydrodynamically controlled process: just like small-molecule LCs, Frank elasticity of the director field provides the restoring torque to a director fluctuation and the LC's viscosity resists the return to equilibrium. Thus, the relaxation rate of homopolymer solutions scales with q^2 (Equation 6.2). Numerous studies on SGLCP solutions have found similar hydrodynamic relaxation and shown that dissolving an SGLCP in a nematic LC increases the viscosity without significantly changing the Frank elastic constants.[4, 17-21]

The dynamical anisotropy observed in homopolymer solutions is consistent with the Brochard theory,[22] which predicts the viscosity to be affected anisotropically depending on the dissolved polymer's conformation in solution: prolate SGLCPs have the greatest effect on the splay viscosity (η_{splay}) while oblate SGLCPs affect the bend viscosity (η_{bend}) more. The end-on homopolymer, which has been shown by small-angle neutron scattering (SANS) to have a mildly oblate conformation in solution with 5CB (Chapter 5), has a greater effect on the dynamics of relaxation in the bend geometry ($\tau / \tau_{5CB} = 120$) than in the splay geometry ($\tau / \tau_{5CB} = 3$). Similarly, the side-on homopolymer has been shown by SANS to adopt a strongly prolate conformation (Chapter 5) and has a larger effect on the dynamics of relaxation in the splay geometry (τ / τ_{5CB} = 90) than in the bend geometry (τ / τ_{5CB} = 3).

The temperature dependence of relaxation dynamics in homopolymer solutions may be interpreted within the Brochard theory to indicate a change in the polymer's conformational anisotropy; the theory predicts the anisotropy in the increase of viscosity to vanish as $R_{||}$ / $R_{\perp}$ approaches unity ($R_{||}$ and $R_{\perp}$ denote the polymer's radii of gyration parallel and perpendicular to the director, respectively). The temperature dependence of end-on homopolymer solution is small, but when side-on homopolymer solution is heated from 31.5 to 33. 5 °C the anisotropy in the relaxation rate, τ_H / τ_V, goes from 60 to 5. This dramatic decrease in dynamical anisotropy is attributed to a decrease in $R_{||}$ / $R_{\perp}$ as the polymer approaches an isotropic conformation near T_{NI} (35 °C). The effect is not evident in end-on polymer where the room-temperature anisotropy is small ($R_{||}$ / $R_{\perp}$ $\approx$ 0.6) compared to that of side-on polymer ($R_{||}$ / $R_{\perp}$ $\approx$ 5-7)[1] and large changes in anisotropy are therefore not possible.

6.4.2 Dynamics of Gels

In contrast to the single hydrodynamic relaxation process observed in homopolymer solutions, relaxation in gels takes place via two distinct processs. The qualitative change in behavior is clearly a consequence of network formation since triblock copolymer solutions below the gel point behave similarly to homopolymers. The gels' fast relaxation process retains the q^2 scaling observed in homopolymer solutions, characteristic of hydrodynamic relaxation, but the slow process has a stronger q dependence and is non-hydrodynamic. The slow process is reminiscent of relaxation dynamics of non-LC physical gels[23-27] but, significantly, light scattering in an LC gel arises from nematic director fluctuations, not from density fluctuations. The LC gels' structural changes are revealed indirectly by their effect on director dynamics. The slow process is attributed to reorganization of the physically associated polymer network: director relaxation via the fast, hydrodynamic process can only proceed to a certain extent because of its coupling to the local orientation of the underlying network. At long times the network structure can rearrange and allow the director to completely lose correlation with its initial orientation.

The proposed mechanism of director relaxation via two processs is illustrated schematically in Figure 6.15. A spontaneous thermal fluctuation causes a distortion to the director field that is translated to the polymer network by the coupling between the director and the network, mediated by the mesogens attached to the polymer midblock. The network distortion causes the local concentration of SGLCP chains to increase or decrease as the crosslinks are pushed together or pulled apart. Relaxation of the distortion takes place by a fast process that does not change the network's connectivity and by a slow restructuring of the network to relieve crowding of adjacent micellar crosslinks and stretching or compressing of chains spanning between two crosslinks. The PS blocks that make up a physical crosslink are constantly disengaging and reengaging, and when one disengages from a crosslink that is in a high energy environment due to polymer crowding or depletion, or chain stretching or compression, it is more likely to reengage in a crosslink that mitigates those osmotic and elastic penalties. The schematic captures the basic physics, but the ordered structure depicted is simply for the sake of clarity. Small-angle neutron scattering from the gel shows no evidence of such long-range order on a cubic lattice.

The dynamical anisotropy that is present in homopolymer solutions translates to the gels, suggesting some anisotropy in the network structure, as well. The SGLCP blocks that make up the network strands have a preferred conformation that balances the alignment of the polymer's mesogens and the director with the backbone's conformational entropy. It is plausible that SGLCPs radiating from a crosslink are, therefore, more likely to connect to another crosslink that is positioned in a way that accommodates that preferred conformation, leading to higher crosslink density perpendicular to the director in the case of end-on polymers and parallel to the director in the case of side-on polymers. This effect also results in an anisotropic distance between crosslinks. The underlying physics for dynamical anisotropy in gels may be understood in terms of the dynamic restructuring of an anisotropic network (Figure 6.16). Distortions to the director field couple to the polymer network and force the physical crosslinks to shift position. The deformation is easily accommodated when the network can undulate along its long axis without significantly changing the average distance between crosslinks. However, when the wavevector of the deformation is along the short axis, crosslinking domains are pushed close together or pulled far apart and the SGLCP network strands are forced to stretch and compress, accordingly. The free energy cost of changing the equilibrium chain conformation, combined with the osmotic resistance to increasing SGLCP overlap, creates a driving force for network rearrangement. Thus, when an end-on gel composed of oblate polymer strands is subjected to a bend distortion, the spreading out and pushing together of crosslink points causes network rearrangement to be an important mechanism for relaxation, but splay distortions are more easily accommodated and relaxation can take place without rearranging the connectivity. The opposite holds true for side-on gels composed of prolate polymer strands where splay distortions more severely perturb the network and bend distortions are relatively easily tolerated. Twist distortions significantly perturb the network in both gels.

Further evidence for anisotropic network structure is found in the temperature dependence of gel relaxation dynamics. The temperature dependence observed in homopolymer solutions carries over to gels: end-on gels are insensitive to temperature, but the relaxation of the side-on gel in the V geometry gets slower with increased temperature, opposite to what is observed in the corresponding homopolymer solution. This is consistent with Lubensky's theory of nematic elastomers,[7] which predicts that the network provides an additional restoring torque on director fluctuations that is highly dependent on its anisotropy. As the side-on gel transitions from being highly anisotropic at low temperature to being mildly anisotropic near T_{NI}, the decrease in the network's restoring torque results in slower relaxation.

6.5 Conclusions

The dynamics of director relaxation in liquid crystalline physical gels are governed by two processes: a fast, hydrodynamic relaxation process similar to homopolymer solutions and a slow relaxation process resulting from the network's ability to rearrange itself. The dynamical anisotropy observed in liquid crystalline gels suggests an anisotropic network structure resulting from the anisotropy of the polymer chains that comprise the network strands. Bend distortions relax slowly in networks composed of oblate polymers because the distortion perturbs the arrangement of the network, but when the polymer chains are prolate, splay distortions are more strongly affected.

The existing theories of LC elastomers and gels[5, 7, 9] cannot be directly applied to a physical gel because the finite lifetime of the crosslinks modifies the director dynamics. An interesting avenue of research would be to combine the theory of LC gels with the theory of associating polymers[28] to predict director dynamics in LC physical gels.

6.6 Tables

Table 6.1 Molecular weight, conversion, and polydispersity of side-group liquid crystal polymers. The full details of characterization are given in Appendix A.

Name	PS Blocks	SGLCP Block				
	M_n [kg/mol]	M_n [kg/mol]	Mole Fraction 1,2 PB	Mole Fraction 1,4 PB	Mole Fraction LC	PDI[a]
490HSiCB4	--	489	0.01	0.03	0.96	1.48
710HSiBB[b]	--	711	0.08	0.03	0.89	1.08
1100ABASiCB4	57,67	1,012	0.02	0.14	0.84	1.16
1400ABASiBB[b]	57,67	1367	0.21	0.14	0.65	1.50

[a] PDI = Polydispersity Index (M_w/M_n)

[b] Synthesized and characterized by Rafael Verduzco[13]

6.7 Figures

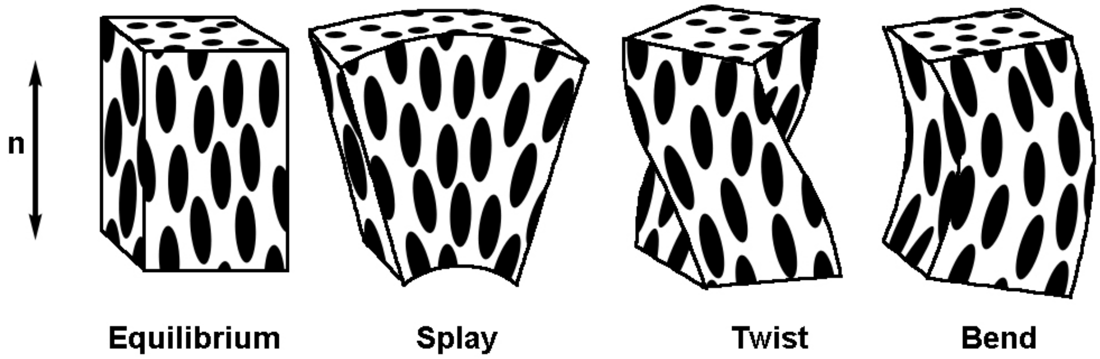

Figure 6.1 Schematic diagrams of the splay, twist, and bend distortions in a nematic liquid crystal. The spatially varying nematic director is represented by ellipses and the equilibrium director is denoted ***n***.

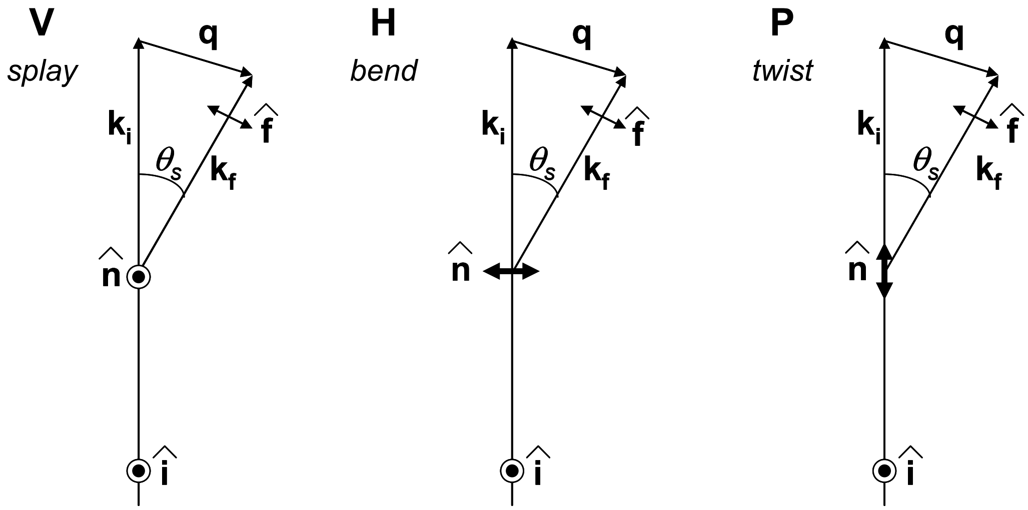

Figure 6.2 Top-view schematic of the three scattering geometries used. The scattering plane, which contains **q**, is in the plane of the page, perpendicular to **i**. Relative to the incident polarization, **i**, and wavevector $\mathbf{k_i}$, the LC director, **n**, is oriented parallel to **i** ("V" for "vertical"), perpendicular to both **i** and $\mathbf{k_i}$ ("H" for "horizontal"), or parallel to $\mathbf{k_i}$ ("P" for "parallel"). The polarization direction of the analyzer, **f**, is horizontal, perpendicular to **i**. The intensity of the scattered, depolarized light is recorded at a discrete angle, θ_s, in the laboratory frame, corresponding to a final wavevector, $\mathbf{k_f}$, and scattering vector $\mathbf{q} = \mathbf{k_f} - \mathbf{k_i}$. The V, H, and P geometries are typically known as the splay, bend, and twist geometries, respectively.

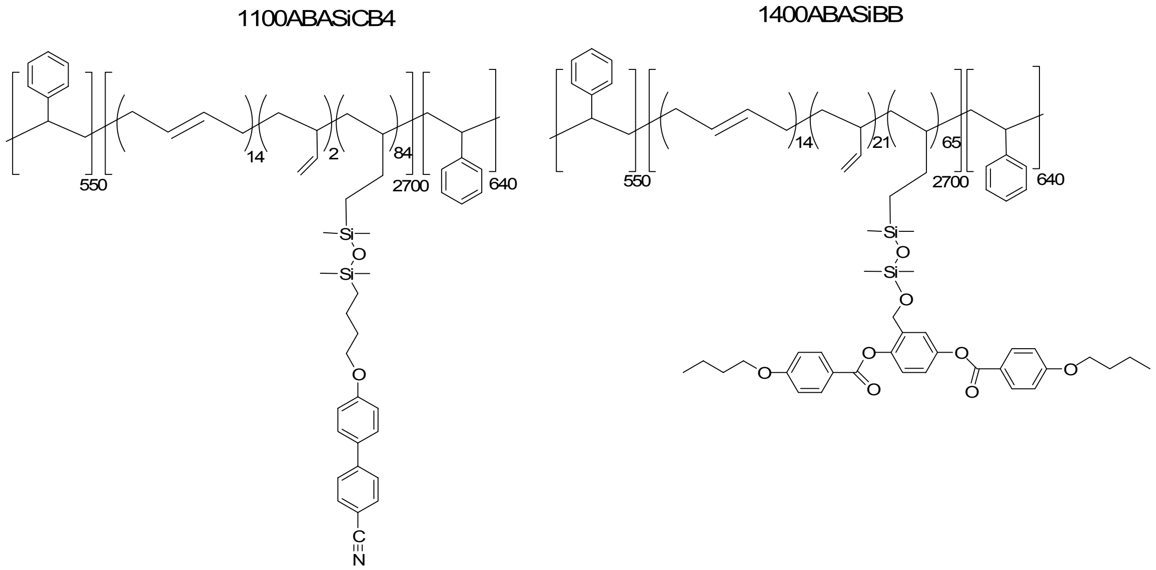

Figure 6.3 Chemical structures of end-on (1100ABASiCB4) and side-on (1400ABASiBB) side-group liquid crystal triblock copolymers with polystyrene endblocks. A polymer's name is derived from its molecular weight in units of kg/mol, the letters "ABA" to indicate a triblock copolymer, and either "SiCB4" or "SiBB" to indicate either end-on or side-on mesogens, respectively. In addition to monomers having an attached mesogen, the midblock also contains some residual 1,2- and 1,4-butadiene monomers. These polymers' properties are summarized in Table 6.1.

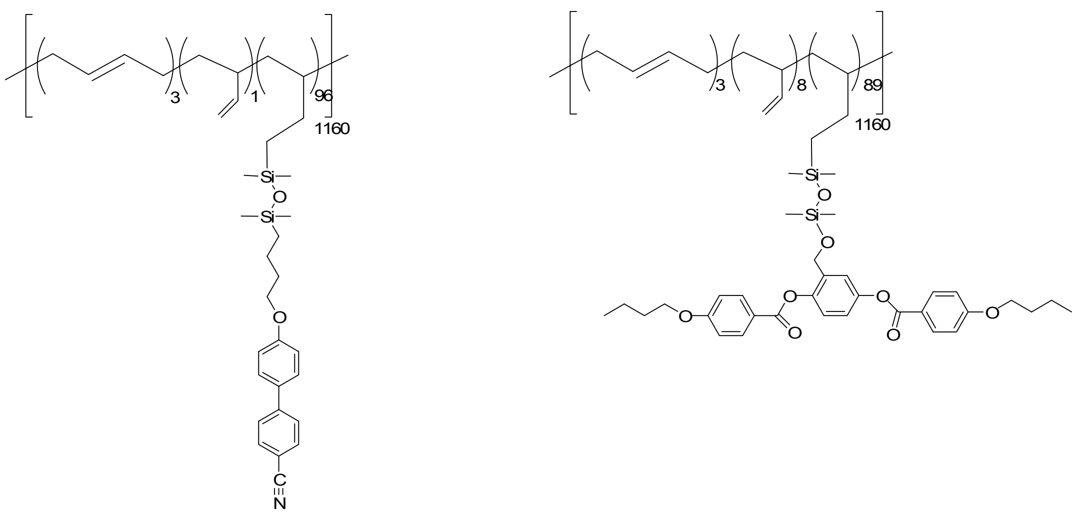

490HSiCB4

710HSiBB

Figure 6.4 Chemical structures of end-on (490HSiCB4) and side-on (710HSiBB) side-group liquid crystal homopolymers. A polymer's name is derived from its molecular weight in units of kg/mol, the letter "H" to indicate a homopolymer, and either "SiCB4" or "SiBB" to indicate either end-on or side-on mesogens, respectively. In addition to monomers having an attached mesogen, the polymer also contains some residual 1,2- and 1,4-butadiene monomers. These polymers' properties are summarized in Table 6.1.

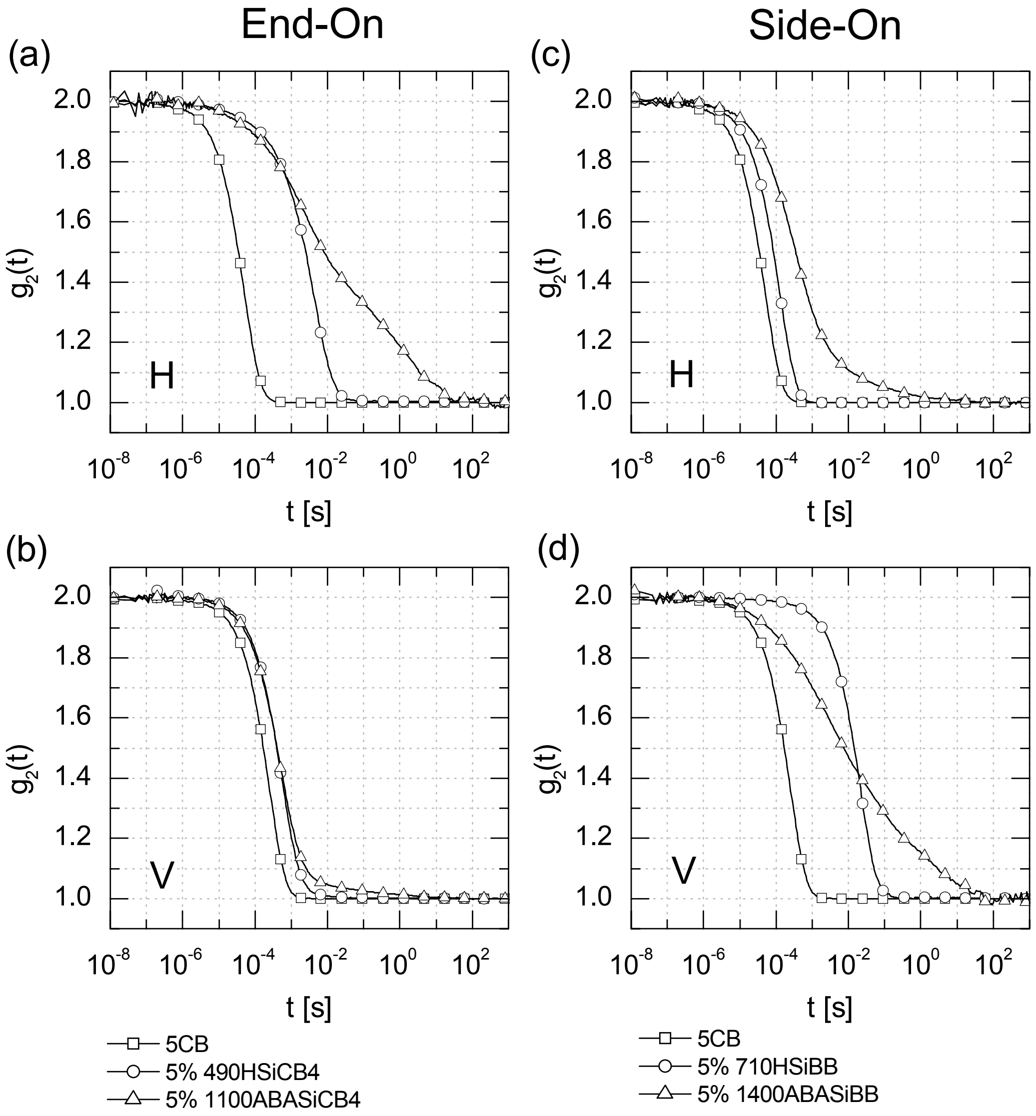

Figure 6.5 Normalized time correlation functions, $g_2(t)$, at 25 °C and $\theta_s = 30°$ for 5CB, 5 wt % homopolymer solutions, and 5 wt % triblock copolymer gels in the H and V orientations

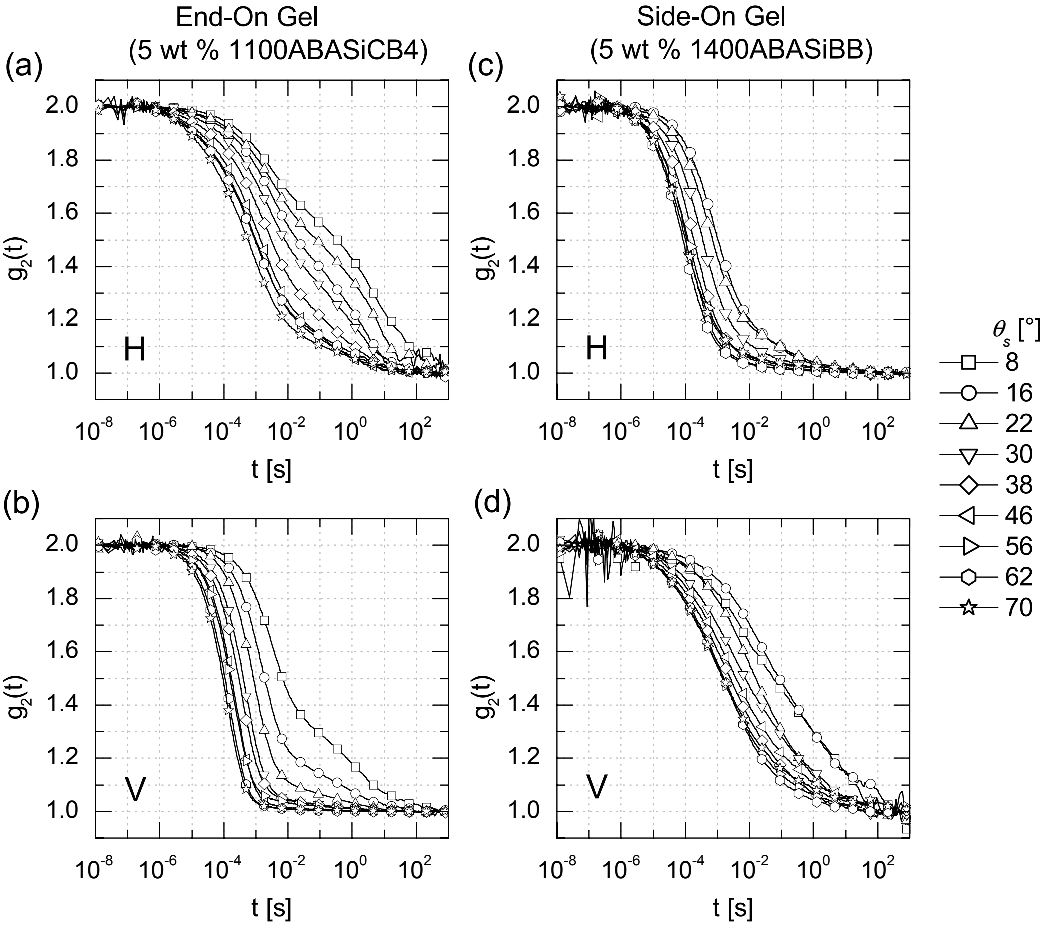

Figure 6.6 Normalized time correlation functions, $g_2(t)$, at 25 °C for end-on and side-on gels (5 wt % 1100ABASiCB4 and 5 wt % 1400ABASiBB, respectively) in the H and V orientations

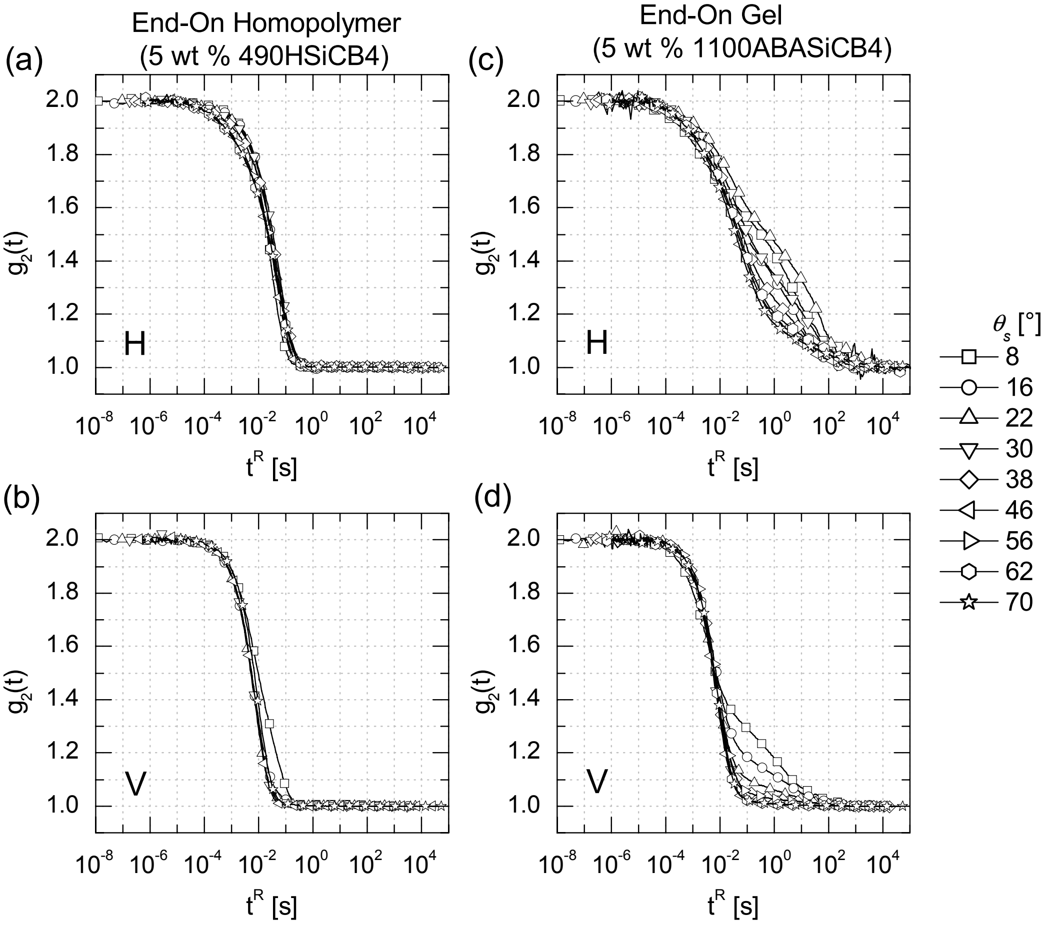

Figure 6.7 Normalized time correlation functions, $g_2(t)$, at 25 °C of end-on polymers at a variety of scattering angles as a function of rescaled delay time, $t^R = t\ (\sin(\theta_s)/\sin(\theta_{s,0}))^2$, where $\theta_{s,0} = 8°$. 5 wt % end-on homopolymer (490HSiCB4) in (a) H orientation and (b) V orientation; and 5 wt % end-on triblock copolymer (1100ABASiCB4) gel in (c) H orientation and (d) V orientation

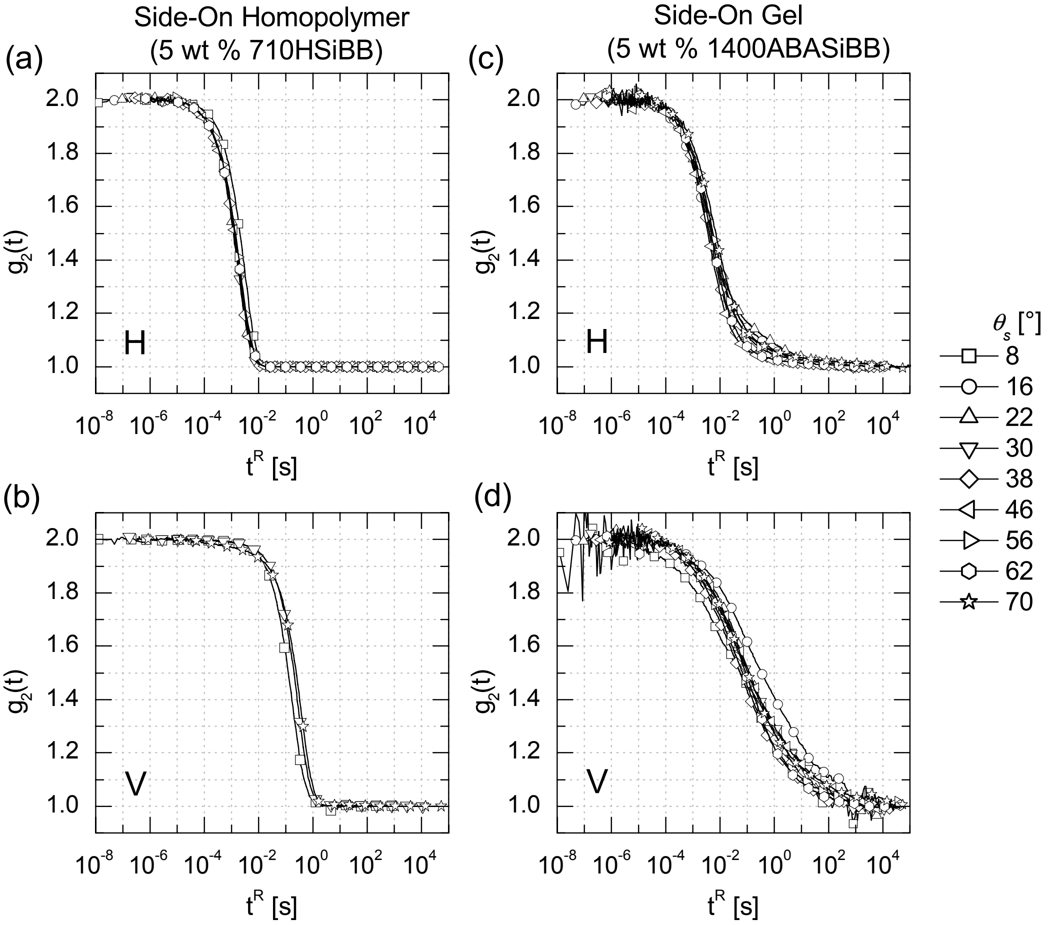

Figure 6.8 Normalized time correlation functions, $g_2(t)$, at 25 °C of side-on polymers at a variety of scattering angles as a function of rescaled delay time, $t^R = t\ (\sin(\theta_s)/\sin(\theta_{s,0}))^2$, where $\theta_{s,0} = 8°$. 5 wt % side-on homopolymer (710HSiBB) in (a) H orientation and (b) V orientation; and 5 wt % side-on triblock copolymer (1400ABASiBB) gel in (c) H orientation and (d) V orientation

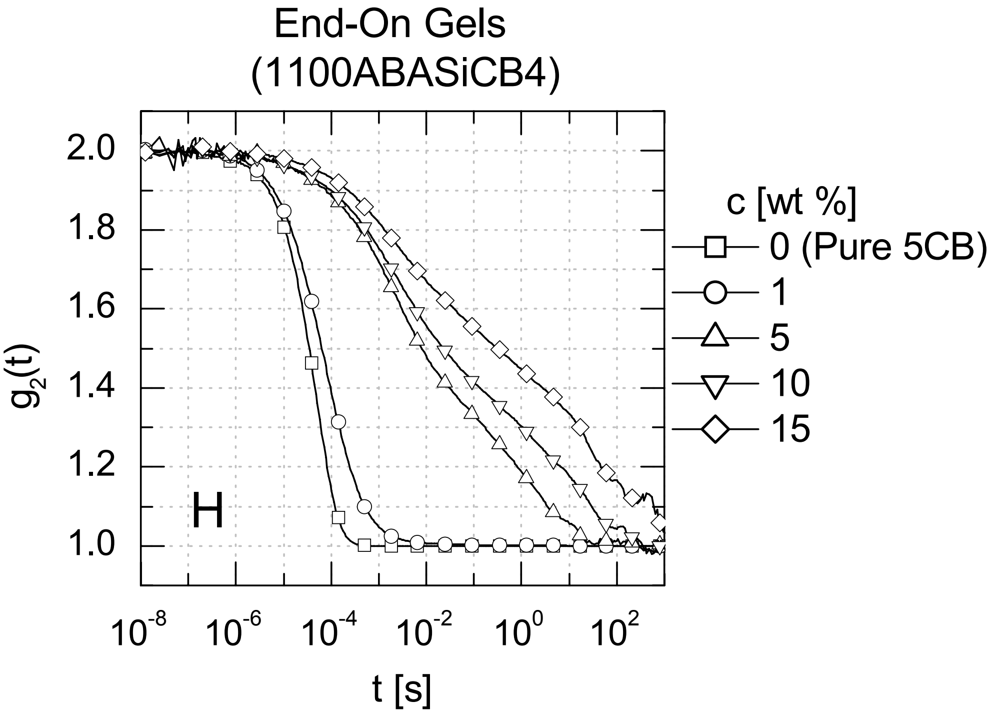

Figure 6.9 Concentration dependence of the normalized time correlation functions, $g_2(t)$, at 25 °C and $\theta_s = 30°$ of end-on triblock copolymer gels (solutions of 1100ABASiCB4) in the H orientation

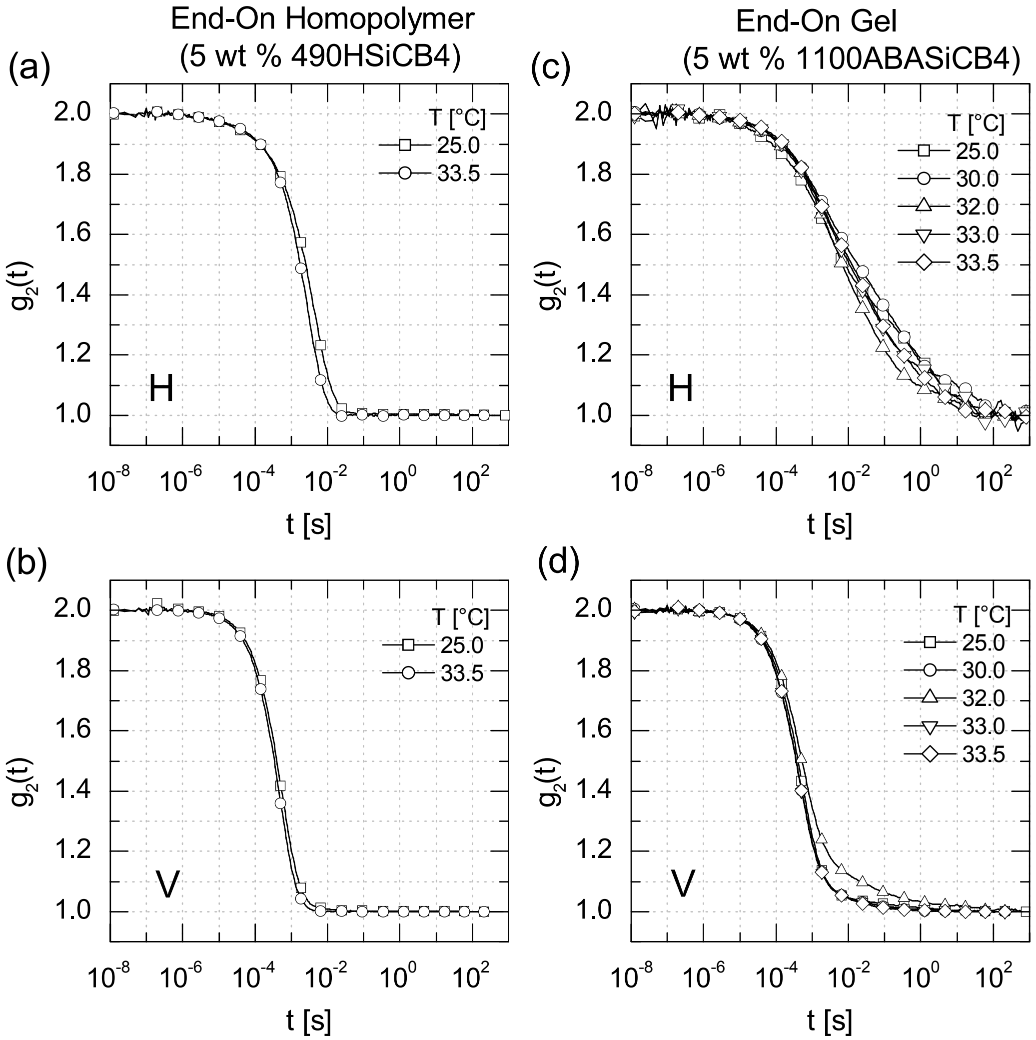

Figure 6.10 Temperature dependence of the normalized time correlation functions, $g_2(t)$, at $\theta_s = 30°$ of 5 wt % end-on homopolymer (490HSiCB4) in (a) H orientation and (b) V orientation and 5 wt % end-on triblock copolymer (1100ABASiCB4) gel in (c) H orientation and (d) V orientation

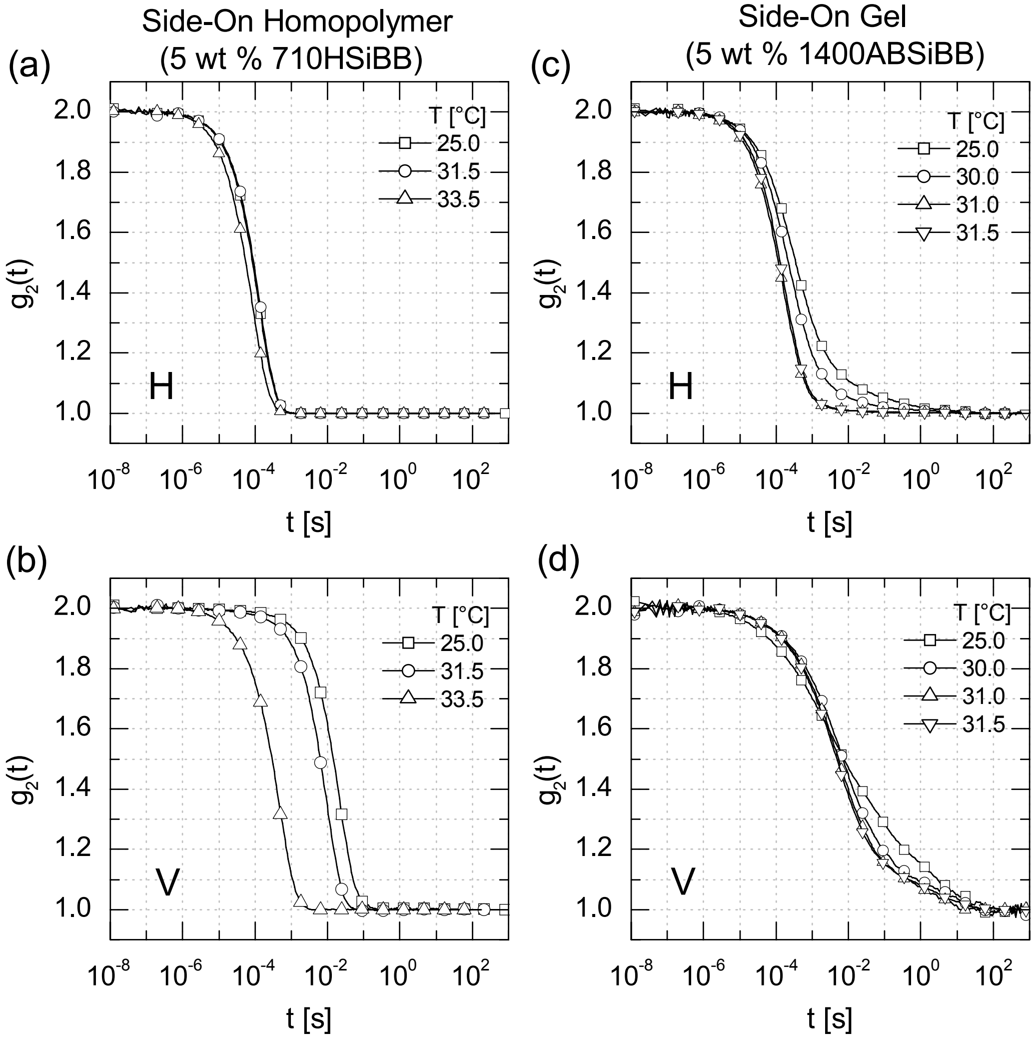

Figure 6.11 Temperature dependence of the normalized time correlation functions, $g_2(t)$, at θ_s = 30° of 5% side-on homopolymer (710HSiBB) in (a) H orientation and (b) V orientation and 5% side-on triblock copolymer (1400ABASiBB) gel in (c) H orientation and (d) V orientation

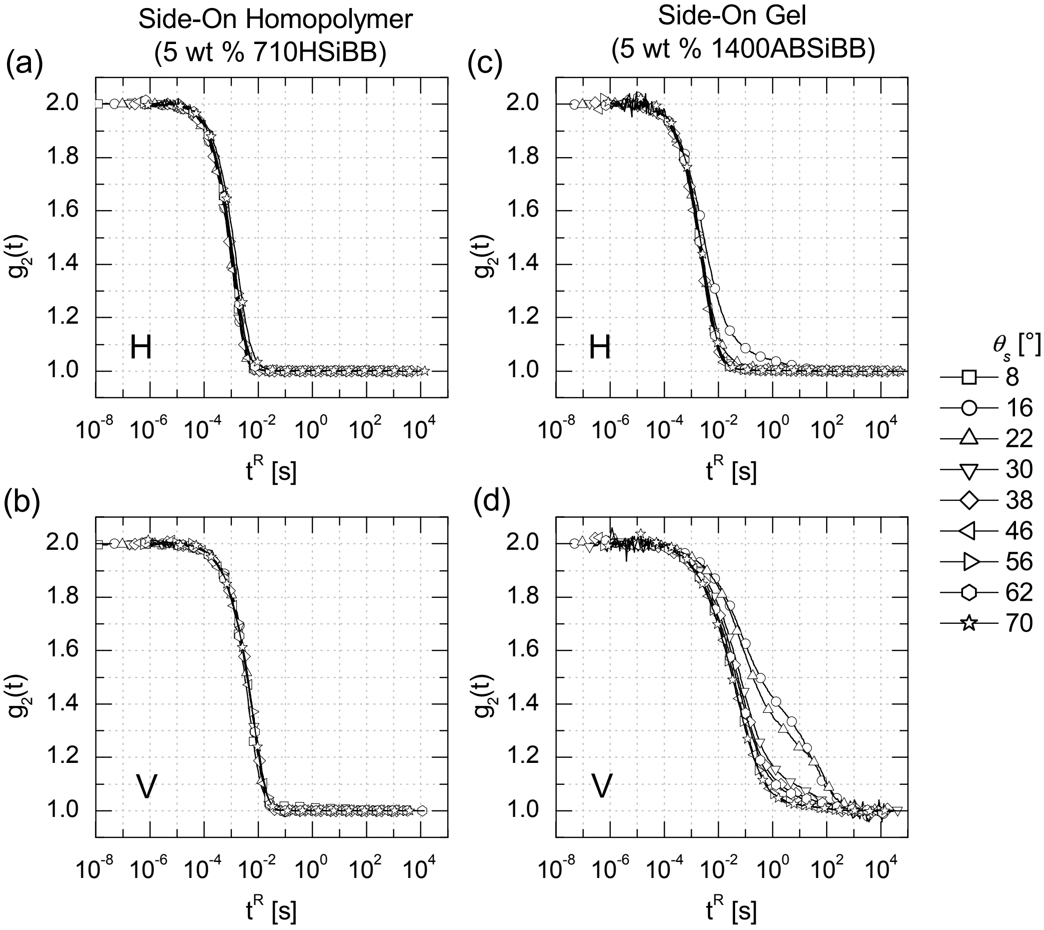

Figure 6.12 Normalized time correlation functions, $g_2(t)$, of side-on homopolymer solution and triblock polymer gel at a variety of scattering angles as a function of rescaled delay time, $t^R = t\ (\sin(\theta_s)/\sin(\theta_{s,0}))^2$, where $\theta_{s,0} = 8°$. 5 wt % side-on homopolymer (710HSiBB) solution at 33.5 °C in (a) H orientation and (b) V orientation and 5 wt % side-on triblock copolymer (1400ABASiBB) gel at 31.5 °C in (c) H orientation and (d) V orientation

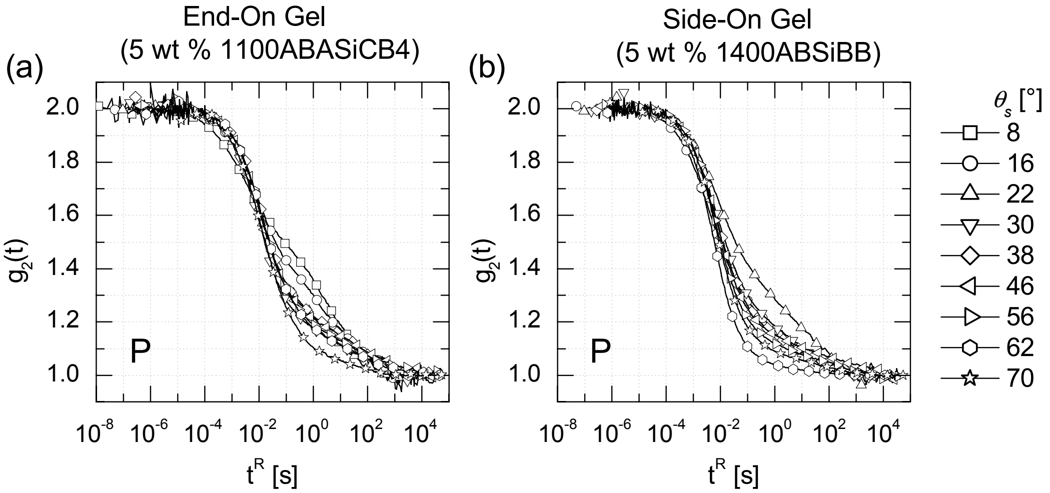

Figure 6.13 Normalized time correlation functions, $g_2(t)$, at 25 °C of triblock copolymer gels in P orientation at a variety of scattering angles as a function of rescaled delay time, $t^R = t\,(\sin(\theta_s)/\sin(\theta_{s,0}))^2$, where $\theta_{s,0} = 8°$. (a) 5 wt % end-on triblock (1100ABASiCB4) and (b) 5 wt % side-on triblock (1400ABASiBB)

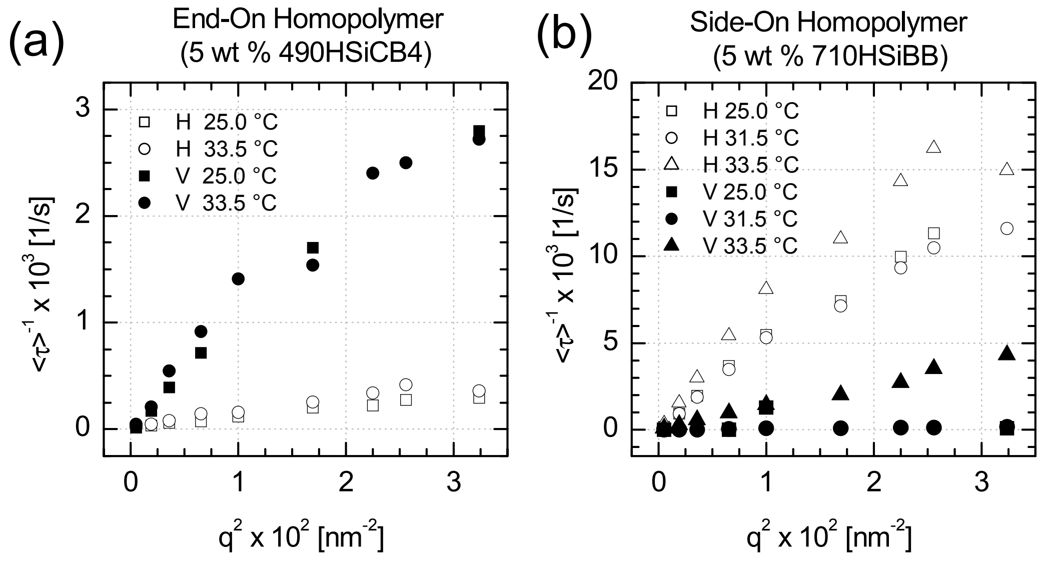

Figure 6.14 Average relaxation rates ($<\tau>^{-1}$) of (a) end-on and (b) side-on homopolymer solutions at various temperatures in the H and V scattering geometries derived from fitting time correlation functions to an empirical Williams-Watts function

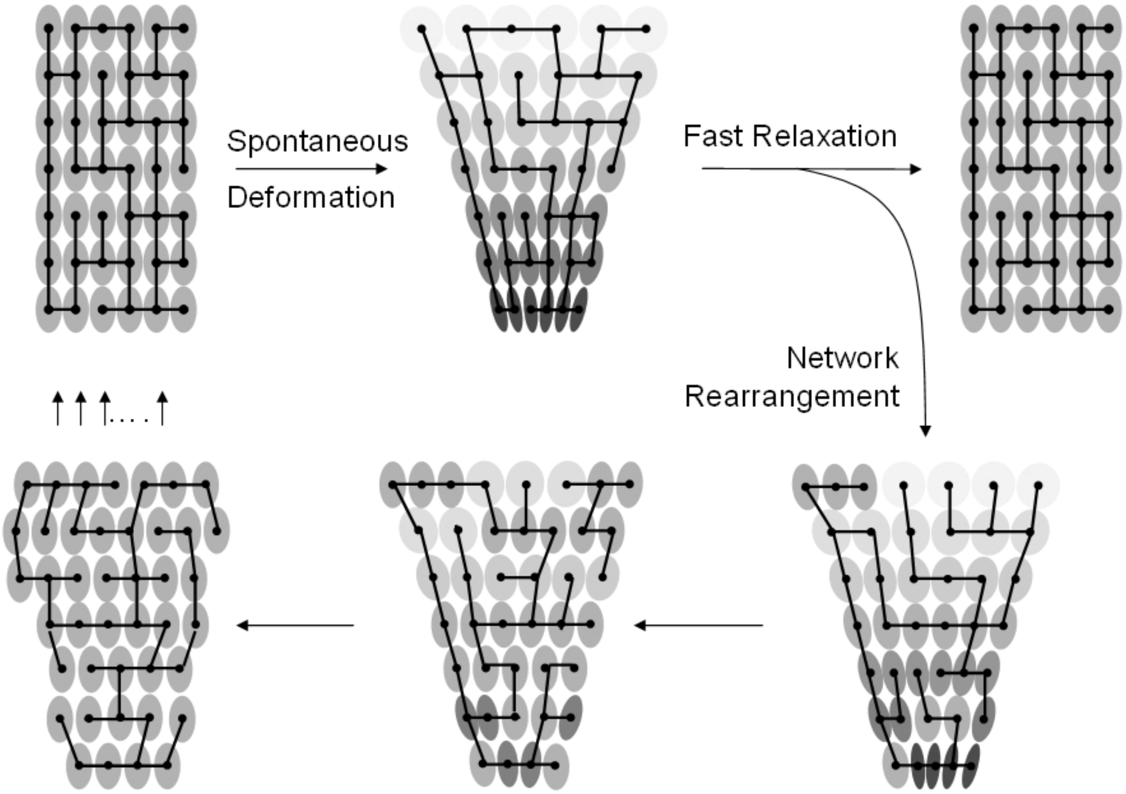

Figure 6.15 Schematic illustrating the two director relaxation processes in LC physical gels. Physical crosslinks consisting of microphase separated polystyrene are represented by black circles and the connections between them, comprised of SGLCP strands, are represented as black lines. The shading of the gray ellipses represents the local density of SGLCP chains. When the network undergoes a spontaneous deformation, it can relax by a fast process that does not require network rearrangement, and by a slow process in which the physical crosslinks break and reform to reestablish a uniform density of SGLCP and mitigate chain stretching.

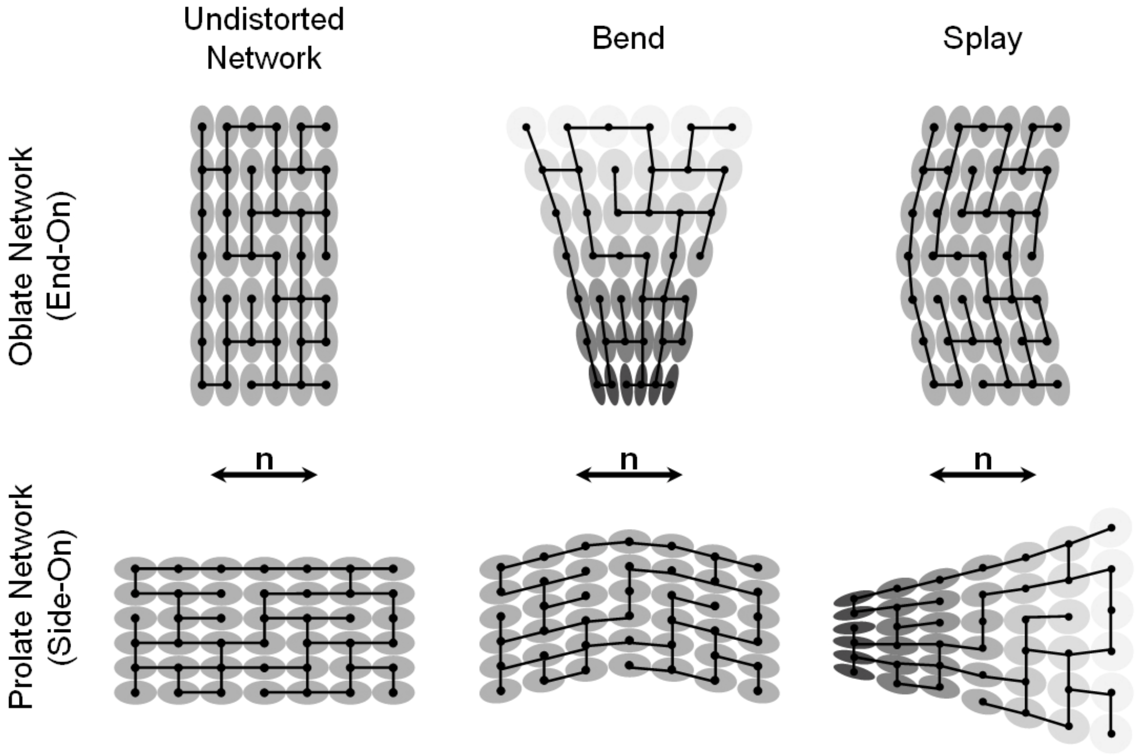

Figure 6.16 Schematic illustrating the effects of bend and splay distortions on an anisotropic network. Physical crosslinks consisting of microphase separated polystyrene are represented by black circles and the connections between them, comprised of SGLCP strands, are represented as black lines. The shading of the gray ellipses represents the local density of SGLCP chains. When an oblate network, such as an end-on LC gel, is subjected to a bend distortion, the local density of SGLCP chains and the average distance between crosslinks are significantly perturbed, but a splay distortion is accommodated by undulation of the network. The effects are reversed in a prolate network, such as a side-on LC gel, where bend distortions are more easily accommodated. The LC director, ***n***, is indicated by the double-headed arrow.

6.8 References

[1] Kempe, M. D.; Scruggs, N. R.; Verduzco, R.; Lal, J.; Kornfield, J. A. Self-assembled liquid-crystalline gels designed from the bottom up. *Nat. Mater.* **2004**, *3*, 177-182.

[2] Ho, J. T. Light scattering and quasielastic spectroscopy. In *Liquid Crystals*; S. Kumar, Editor; Cambridge University Press: Cambridge, 2001.

[3] de Gennes, P.-G. *The Physics of Liquid Crystals*, 2nd ed; Clarendon Press: Oxford, 1993.

[4] Jamieson, A. M.; Gu, D. F.; Chen, F. L.; Smith, S. Viscoelastic behavior of nematic monodomains containing liquid crystal polymers. *Prog. Polym. Sci.* **1996**, *21*, 981-1033.

[5] Warner, M.; Terentjev, E. M. Nematic elastomers- a new state of matter? *Prog. Polym. Sci.* **1996**, *21*, 853-891.

[6] Olmsted, P. D. Rotational invariance and Goldstone modes in nematic elastomers and gels. *J. Phys. II France* **1994**, *4*, 2215-2230.

[7] Stenull, O.; Lubensky, T. C. Dynamics of nematic elastomers. *Phys. Rev. E* **2004**, *69*, 051801.

[8] Terentjev, E. M.; Warner, M. Linear hydrodynamics and viscoelasticity of nematic elastomers. *Eur. Phys. J. E* **2001**, *4*, 343-353.

[9] Warner, M.; Terentjev, E. M. *Liquid Crystal Elastomers*, Oxford University Press: Oxford, 2003.

[10] Schöenstein, M.; Stille, W.; Strobl, G. Effect of the network on the director fluctuations in a nematic side-group elastomer analysed by static and dynamic light scattering. *Eur. Phys. J. E* **2001**, *5*, 511-517.

[11] Kempe, M. D.; Verduzco, R.; Scruggs, N. R.; Kornfield, J. A. Rheological study of structural transitions in triblock copolymers in a liquid crystal solvent. *Soft Matter* **2006**, *2*, 422-431.

[12] Verduzco, R.; Meng, G.; Kornfield, J. A.; Meyer, R. B. Buckling instability in liquid crystalline physical gels. *Phys. Rev. Lett.* **2006**, *96*, 147802.

[13] Verduzco, R. Texture Transitions, Electro-Optics, and Dynamics of Liquid Crystal Gels with Novel Network Architectures. Ph.D. Thesis, California Institute of Technology, Pasadena, CA, February 5, 2007.

[14] Williams, G.; Watts, D. C. Non-Symmetrical Dielectric Relaxation Behaviour Arising from a Simple Empirical Decay Function. *Trans. Faraday Soc.* **1970**, *66*, 80-85.

[15] Williams, G.; Watts, D. C.; Dev, S. B.; North, A. M. Further Considerations of Non Symmetrical Dielectric Relaxation Behaviour arising from a Simple Empirical Decay Function. *Trans. Faraday Soc.* **1977**, *67*, 1323-1335.

[16] Lindsey, C. P.; Patterson, G. D. Detailed comparison of the Williams-Watts and Cole-Davidson functions. *J. Chem. Phys.* **1980**, *73*, 3348-3357.

[17] Gu, D. F.; Jamieson, A. M.; Kawasumi, M.; Lee, M.; Percec, V. Dynamic Light Scattering from Nematic Monodomains Containing Mesogenic Polymers of Differing Architectures. *Macromolecules* **1992**, *25*, 2151-2155.

[18] Gu, D. F.; Jamieson, A. M.; Rosenblatt, C.; Tomazos, D.; Lee, M.; Percec, V. Dynamic Light Scattering from a Nematic Monodomain Containing a Side-Chain Liquid Crystal Polymer in a Nematic Solvent. *Macromolecules* **1991**, *24*, 2385-2390.

[19] Chiang, Y.-C.; Jamieson, A. M.; Campbell, S.; Tong, T. H.; Sidocky, N. D.; Chien, L. C.; Kawasumi, M.; Percec, V. Electro-rheological behavior of liquid crystal polymers dissolved in a nematic solvent: dependence on temperatrue and LCP structure. *Polymer* **2000**, *41*, 4127-4135.

[20] Chiang, Y.-C.; Jamieson, A. M.; Campbell, S.; Lin, Y.; O'Sidocky, N.; Chien, L. C.; Kawasumi, M.; Percec, V. Effect of molecular architecture on the electrorheological behavior of liquid crystal polymers in nematic solvents. *Rheological Acta* **1997**, *36*, 505-512.

[21] Chen, F.-L.; Jamieson, A. M.; Kawasumi, M.; Percec, V. Viscoelastic properties of dilute nematic mixtures containing cyclic and hyperbranched liquid crystal polymers dissolved in a nematic solvent. *Journal of Polymer Science: Part B: Polymer Physics* **1995**, *33*, 1213-1223.

[22] Brochard, F. Viscosities of Dilute Polymer-Solutions in Nematic Liquids. *J. Polym. Sci. Pt. B-Polym. Phys.* **1979**, *17*, 1367-1374.

[23] Blanco, M. C.; Leisner, D.; Vazquez, C.; Lopez-Quintela, M. A. Dynamic Light Scattering in Transient Reversible Gels. *Langmuir* **2000**, *16*, 8585-8594.

[24] Castelletto, V.; Hamley, I. W.; Waigh, T. A. Dynamic light scattering study of the dynamics of a gelled polymeric micellar system. *J. Chem. Phys.* **2004**, *121*, 11474-11480.

[25] Konak, C.; Fleischer, G.; Tuzar, Z.; Bansil, R. Dynamics of Solutions of Triblock Copolymers in a Selective Solvent: Effect of Varying Copolymer Concentration. *J. Polym. Sci., Part B: Polym. Phys.* **2000**, *38*, 1312-1322.

[26] Konak, C.; Helmstedt, M.; Bansil, R. Dynamics in Solutions of Associating Statistical Copolymers. *Macromolecules* **1997**, *30*, 4342-4346.

[27] Raspaud, E.; Lairez, D.; Adam, M.; Carton, J.-P. Triblock Copolymers in a Selective Solvent. 2. Semidilute Solutions. *Macromolecules* **1996**, *29*, 1269-1277.

[28] Tanaka, F. Theoretical Study of Molecular Association and Thermoreversible Gelation in Polymers. *Polym. J. (Tokyo, Jpn.)* **2002**, *34*, 479-509.